considered in FHN. We give below the final formula, omitting details of the calculations:

$$\frac{\nu_{\text{source}}}{\nu_{\text{reception}}}=\left(1-\frac{R_c}{R_i}\frac{R_i}{R}\right)^{1/2}\Bigg/\left\{\left(1-\frac{R_c}{R_i}\right)^{1/2}+\left[\frac{R_c}{R_i}\left(\frac{1}{s}-1\right)\right]^{1/2}\right\}, \quad (17)$$

where the symbols have the same meanings as in FHN. Some trial calculations show that the calculated values from (17) agree with the values given in FHN, even when the surface is well inside the Schwarzschild radius. This is interesting for in our deduction we have utilized the Schwarzschild line element, the applicability of which seems questionable for $\xi^2<2m$.

V. CONCLUDING REMARKS

Our formulas have been deduced on the hypothesis of a homogeneous dust system. Should one introduce nonhomogeneity and pressure, the results would surely be quantitatively different although the general features would apparently be preserved.

ACKNOWLEDGMENTS

The author is deeply indebted to Professor A. K. Raychaudhuri of Presidency College, Calcutta for his continuous help and useful guidance.

PHYSICAL REVIEW VOLUME 150, NUMBER 4 28 OCTOBER 1966

Production of Low-Energy Cosmic-Ray Electrons

P. B. ABRAHAM, K. A. BRUNSTEIN,* AND T. L. CLINE
Goddard Space Flight Center, Greenbelt, Maryland
(Received 16 May 1966)

The production of cosmic-ray electrons of characteristically low energies is investigated. Secondary sources, other than that of meson decay, are considered, and constraints are placed on both secondary and primary sources. (1) Calculations are made of the intensity of low-energy knock-on and beta-decay electrons which are secondary to cosmic-ray interactions. In particular, knock-on production is calculated in the 100-KeV to 50-BeV kinetic-energy interval. Interstellar losses due to ionization, leakage from the galaxy, and synchrotron, bremsstrahlung, and inverse Compton effects are considered, as well as those due to plasma excitation, the red shift and synchrotron, bremsstrahlung, and inverse Compton effects in the intergalactic medium. The intensity of low-energy relativistic electrons from these sources is not negligible compared with the low energy $\pi\rightarrow\mu\rightarrow e$ intensity, but it is shown not to account for the observed interplanetary electron intensity. (2) Energy inputs to the injected secondary electrons by a possible solar electric field of low magnitude and by a possible galactic Fermi acceleration are investigated. It is shown that at least one such input is necessary if the observed low-energy interplanetary electron intensity is to be attributed to secondary production alone. A heliocentric field which does allow for a fit to the low-energy data cannot, however, account for the high-energy BeV electrons found to be in excess of those from $\pi\rightarrow\mu\rightarrow e$ production. The Fermi acceleration shown to be necessary to provide a fit is greater than that usually postulated for cosmic-ray protons, and also requires that the ratio of escape losses to acceleration λ/α be much smaller than is usually assumed for protons. This distinction is acceptable only if one postulates a significant difference between interstellar proton and electron propagation. (3) The observation that the velocity spectrum of electrons in the energy-per-unit-mass region of 7–25 closely approximates that of the cosmic-ray protons, and the necessity of constraints on the secondary-electron hypothesis outlined above, suggest that most of the low-energy electrons are of primary origin. The similarity between this conclusion and the conclusion (based on the measurement of the charge ratio of electrons) that the higher energy electrons are mostly primary is discussed.

I. INTRODUCTION AND DISCUSSION OF OBSERVATIONS

THE study of cosmic radiation has been, for the most part, the measurement of the intensities and energy spectra of the protons and other nuclei which possess the bulk of the cosmic-ray energy content. Recently, the electromagnetic component began to be investigated: Earl[1] and Meyer and Vogt[2] found electrons which have typical cosmic-ray energies, but which, in the BeV region, have only a small fraction of the proton intensity. Also, DeShong, Hildebrand, and Meyer[3] later found that the electron flux is partially composed of positrons. In addition, Kraushaar *et al.*[4] set a new upper limit to the high-energy gamma-ray intensity. Since one can assume that some of these electrons and gamma rays may be primary cosmic rays and

* National Academy of Sciences—National Aeronautics and Space Administration post-doctoral research associate.
[1] J. A. Earl, Phys. Rev. Letters **6**, 125 (1961).
[2] P. Meyer and R. Vogt, Phys. Rev. Letters **6**, 193 (1961).
[3] J. A. DeShong, R. H. Hildebrand, and P. Meyer, Phys. Rev. Letters **12**, 3 (1964).
[4] W. L. Kraushaar, G. W. Clark, G. Garmire, H. Helmken, P. Higbie, and M. Agogino, Astrophys. J. **141**, 845 (1965).

some may be secondary to cosmic-ray interactions, it follows that a great deal of new information about the origins and behavior of cosmic rays in the galaxy might come from a study of these rarer components. Most recently, a component of relativistic electrons in the few-MeV energy region was found in interplanetary space by Cline, Ludwig, and McDonald.[5] If we assume, as a working hypothesis, that the electrons of these extremely low energies are also of cosmic origin, we may learn something more by comparing their properties with those of the higher energy electrons, protons and other cosmic rays. It is the purpose of this paper to discuss the possible sources of these particles.

Cosmic rays are presumably created when very low energy particles are injected into some region where they are then accelerated; if this region is not interstellar space itself, they may temporarily be stored in or near that region before propagating through the galaxy; finally they are modulated in the solar environment before being detected. Certainly, several processes may compete for production, and others may take place in uncertain chronological order. The most fundamental model of interstellar acceleration, introduced by Fermi,[6] and the most quantitative model of solar modulation, described by Parker,[7] and combinations and variations of these, may possibly describe a great share of cosmic-ray origin and propagation. Since Fermi's model depends only on the particle's total energy per unit mass, which is a function of velocity (independent of charge or mass), and since Parker's model also depends on velocity alone at asymptotically low-particle rigidity, we choose to represent all quantities in terms of the total energy per unit rest-mass energy, γ.

The first measurements of the low-energy electrons are shown in Fig. 1, in which the intensity, $(dJ/d\gamma_e)$, is plotted versus γ. These particles were found in interplanetary space with Explorer XVIII. The argument supporting a nonlocal origin of the electrons, put forth by the observers, rests on the fact that they undergo systematic intensity modulations of greater magnitude than any possible cosmic-ray parent component. The actual intensity is uncertain, since some fraction of the steady or baseline intensity may be local or instrumental; thus, the true intensity is between the magnitude of a typical modulated increase and the total magnitude of baseline plus the increase. Both the steady and incremental intensities are shown in the figure: a typical increase is apparently energy-independent and is about 50% the steady value.

Also shown are the electron measurements in the higher energy region: not all observations known are included, but those are displayed that are the only

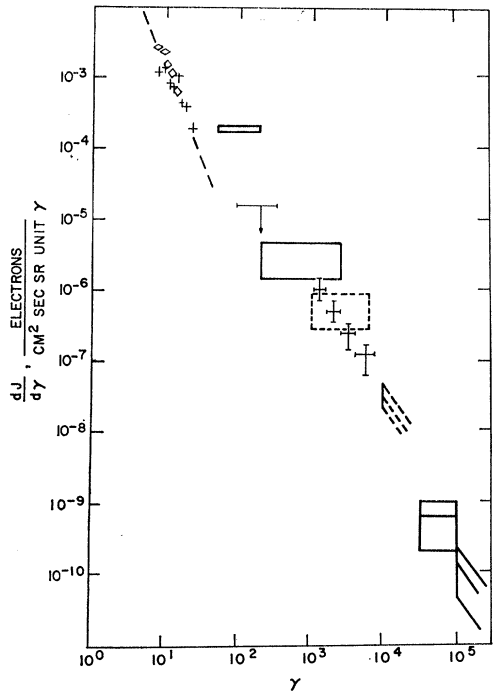

FIG. 1. Observed cosmic-ray electron intensities in the $1<\gamma<10^6$ region. Most of the differential intensities shown are taken directly from the references [Cline, Ludwig, and McDonald (Ref. 5), in which the diamonds represent steady values and the crosses time variations; Schmoker and Earl (Ref. 8); Meyer and Vogt (Ref. 2); Earl (Ref. 1); L'Heureux and Meyer (Ref. 11)]. The integral intensities of Agrinier *et al.* (Ref. 9) and Daniel and Stephens (Ref. 10) were converted to differential intensities by assuming a slope of -1.5 and an infinitely high cutoff.

data available in a given energy interval,[8–10] the most recent data with the best statistics,[11] or the original data.[1,2] It is inferred from the measurements on the position-to-electron ratio[3,12] that approximately one third to two thirds of the electrons in the 1-BeV region are from a source other than $\pi \rightarrow \mu \rightarrow e$ decay. Since we can expect that the $\pi \rightarrow \mu \rightarrow e$ differential spectrum peaks in the $20<\gamma<200$ region, all of the very low energy electrons must be from another source. The more recently obtained higher energy data can be fitted to a common curve, but it departs from the low-energy fit, shown in Fig. 1 as a dashed line, by an amount between one and two orders of magnitude at the high energies, where $\gamma>1000$. Whether, after the $\pi \rightarrow \mu \rightarrow e$ component has been subtracted out, the remaining spectrum is of one smooth form, or is the sum of two or more separate spectra, cannot be determined until after the differential intensities in the $10<\gamma<100$ and $\gamma>10^4$

[5] T. L. Cline, G. H. Ludwig, and F. B. McDonald, Phys. Rev. Letters **13**, 286 (1964).
[6] E. Fermi, Phys. Rev. **75**, 1169 (1949).
[7] E. N. Parker, *Interplanetary Dynamical Processes* (Interscience Publishers, Inc., New York, 1963).
[8] J. W. Schmoker and J. A. Earl, Phys. Rev. **138**, B300 (1965).
[9] B. Agrinier, Y. Koechlin, B. Parlier, G. Boella, G. Degli Antoni, C. Dilworth, L. Scarsi, and G. Sironi, Phys. Rev. Letters **13**, 377 (1964).
[10] R. R. Daniel and S. Z. Stephens, Phys. Rev. Letters **15**, 769 (1965).
[11] J. L'Heureux and P. Meyer, Phys. Rev. Letters **15**, 93 (1965).
[12] R. C. Hartman, P. Meyer, and R. H. Hildebrand, J. Geophys. Res. **70**, 2713 (1965).

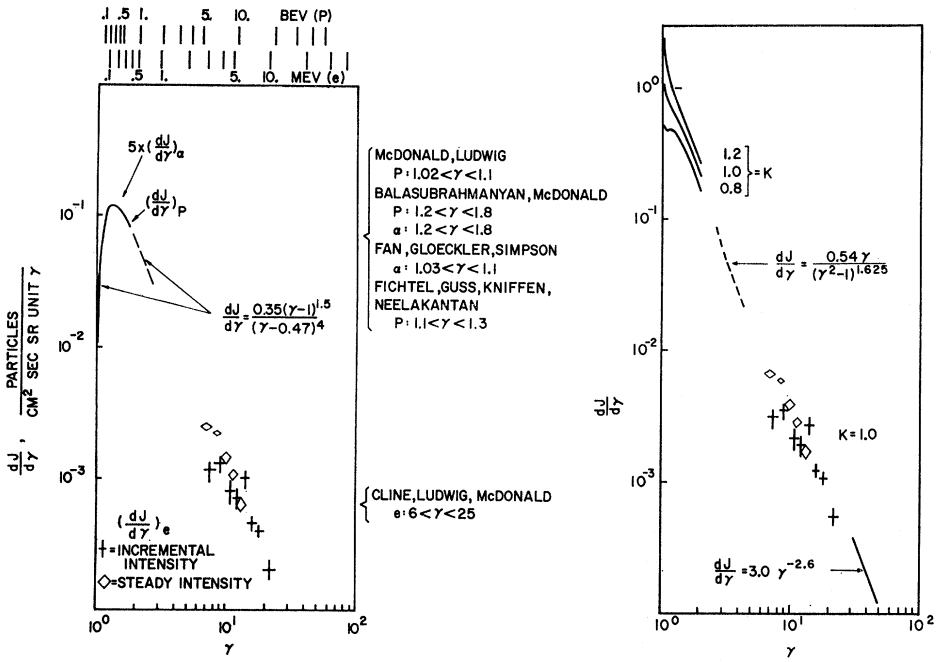

FIG. 2. (a) The low-energy electron observations plotted, for comparison, with a smooth fit to a composite of the low-energy proton and alpha data, in which the alpha intensities have been multiplied by 5. The dashed curve is an extrapolation, beyond the measurements, of the proton and alpha fit, devised by Balasubrahmanyan, Boldt, and Palmeira (Ref. 17). (b) The same data, for which the proton curve has been demodulated by the factor $\exp(K/\beta)$ with three values of K and for which the electron data have been altered with $K=1$. Higher energy proton fits [McDonald and Webber (Ref. 28), Ginsburg and Syrovatskii (Ref. 22)] are shown for comparison. These curves were taken from Brunstein and Cline (Ref. 18).

regions are known and after the $\pi \rightarrow \mu \rightarrow e$ component itself is accurately determined by calculation and measurement of the e^+/e^- ratio. The sources of the electrons of $\gamma \lesssim 50$ most likely pose a quite separate question from that of the higher energy electrons. The very low energy electrons are shown again in Fig. 2(a) compared with a representation of the composite primary cosmic-ray proton intensity, observed by McDonald, and Ludwig,[13] and the primary alpha-particle intensity, observed by Fan, Gloeckler, and Simpson.[14] These electron, proton, and alpha measurements, made on the same satellite, are shown together with balloon measurements by Balasubrahmanyan and McDonald[15] and by Fichtel, Guss, Kniffen, and Neelakantan.[16] The proton and alpha intensities fit a common curve when the alpha values are multiplied by a constant factor of ≈ 5, to take into account the relative abundances. This composite representation of the 1963 proton and alpha spectra, which was introduced recently by Balasubrahmanyan, Boldt, and Palmeria[17] fits the data all the way through this low-energy region; adapted to our units, it is

$$dJ/d\gamma = 0.35(\gamma-1)^{1.5}(\gamma-0.47)^{-4}$$

particles/cm² sec sr (unitγ).

The similarity between the observed electron and proton differential velocity spectra has been discussed in a paper by Brunstein and Cline,[18] from which this figure was taken. They point out that after solar demodulation is taken into account by use of the model of Parker[7] the electrons and protons fit even more closely the same spectrum, as shown in Fig. 2(b). The fact that this spectrum is a simple power law in total energy, which, for the protons at least, is continuous from a nonrelativistic γ of 1.02 up to the extreme relativistic region, is suggestive of a Fermi acceleration. However, the fact that this fit is accomplished *before* the usual correction for the 2.5-g cm^{-2} galactic path length is made, means that either it is accidental or that electrons and protons may indeed be propagated with spectral neutrality over a wide energy range. As outlined by Brunstein and Cline,[18] several possibilities present themselves; low-energy electrons and protons may be Fermi-accelerated from neutral material in the galactic medium in such a manner as to overcompensate ionization losses, or the 2.5-g cm^{-2} path with its attendant spectral alteration and fragmentation probabilities may apply only to the heavies, or the electrons and protons may have a metagalactic origin, in which case during their travel to the solar system they encounter very little material. It is clear that these questions cannot at present be answered. What we will investigate in this paper is the possibility that the low-energy electrons are secondary to galactic cosmic rays, and the relation of this possibility to the question of a primary electron source.

[13] F. B. McDonald and G. H. Ludwig, Phys. Rev. Letters **13**, 783 (1964).

[14] C. Y. Fan, G. Gloeckler, and J. A. Simpson, University of Chicago Report No. EFINS, 65-22, 1965 (unpublished).

[15] V. K. Balasubrahmanyan and F. B. McDonald, J. Geophys. Res. **69**, 3289 (1964).

[16] C. E. Fichtel, D. E. Guss, D. A. Kniffen, and K. A. Neelakantan, J. Geophys. Res. **69**, 3293 (1964).

[17] V. K. Balasubrahmanyan, E. A. Boldt, and R. A. R. Palmeira, Phys. Rev. **140**, B1157 (1965).

[18] K. A. Brunstein and T. L. Cline, Nature **209**, 1186 (1966).

Hayakawa and Okuda[19] originally suggested that high-energy electrons should arise from $\pi \rightarrow \mu \rightarrow e$ decay following meson production in collisions of cosmic rays with the interstellar gas. Their calculations, and those of Jones,[20] Pollack and Fazio,[21] Ginzburg and Syrovatskii,[22] Gould and Burbidge,[23] and others showed that indeed a certain fraction of the observed electrons of $\gamma \gtrsim 50$ may originate in this manner. The high-energy positron-to-electron ratio, found by DeShong *et al.*[3] and by Hartman *et al.*[24] to be low, indicates the less than half of the observed electrons in the $\gamma \gtrsim 200$ region are secondaries from this process. Brunstein[25] showed that Coulomb collisions could similarly account for only a fraction of the observed electrons with $5 < \gamma < 50$ unless a Fermi-like post-acceleration was incorporated. The origin of the majority of electrons in all observed energy regions is therefore tentatively unexplained. In the calculations that follow we investigate in detail some of the various production mechanisms which may be responsible.

II. SECONDARY GALACTIC ELECTRONS

A. Knock-On Electrons

The most certain process by which cosmic rays can produce low-energy relativistic electrons through interactions with the interstellar medium is that of Coulomb collisions. In this process, energy is transferred to an atomic electron in great excess of its binding energy, and it recoils in billiard-ball fashion; free plasma electrons are turned into cosmic-ray secondaries in the traversal of cosmic rays through the galactic medium in the same fashion.

We use the cross section for knock-on production calculated by Bhabha.[26] The particular form of the cross section we incorporate is that for spin $\frac{1}{2}$, in order to obtain quantitatively accurate results to very high energies, $\gamma \approx 10^5$ or 10^6. (The form used by Brunstein[25] was for spin 0 but was sufficiently accurate for the $5 \lesssim \gamma \lesssim 50$ region.) The differential probability for the production of an electron having total energy per unit rest-mass energy in $d\gamma_e$ at γ_e by the collision of a cosmic ray of particle species j having the energy factor γ_j with a target of charge Z_i and atomic number A_i is

$$\Phi_i(\gamma_e,\gamma_j)d\gamma_e = \left\{ \frac{2\pi N_0 Z_i r_e^2 Z_j^2}{A_i(1-\gamma_j^{-2})} \times \left\{ \frac{1}{(\gamma_e-1)^2} - \frac{s\left(\gamma_j + \frac{s+1/s}{2}\right)}{(\gamma_e-1)\gamma_j^2} + \frac{s^2}{2\gamma_j^2} \right\} \right\} d\gamma_e \text{ cm}^2/\text{g}, \quad (1)$$

in which N_0 is Avogadro's number, r_e is the classical radius of the electron: $r_e = e^2/mc^2 = 2.82 \times 10^{-13}$ cm, and $s = m_e/(A_i m_p)$. and for which the maximum transferable energy is

$$\gamma_{\max} = 1 + (\gamma_j^2 - 1) \Big/ \left(s\left\{ \gamma_j + \frac{s+1/s}{2} \right\} \right). \quad (2)$$

We make the usual approximation that the elemental abundances in the interstellar medium relative to hydrogen a_i can be represented by taking that of helium to be about 0.10 and by ignoring the higher Z components. This approximation introduces a negligible error, particularly since the probability varies only as Z_i/A_i to the first power. The contributions by the various nuclear species in the cosmic radiation are more important, varying as the square of Z_j. Using the cosmic-ray abundances relative to protons (b_j) given by Ginzburg and Syrovatskii,[27] we estimate that the total contribution from primaries of charge $Z_j \geq 2$ will be about an additional 0.75. Thus, $s \approx 1/1836$, and

$$\Phi(\gamma_j) = \sum_i \frac{a_i Z_i}{A_i} \sum_j b_j Z_j^2 \Phi(\gamma_i) \approx 1.75 \Phi_1(\gamma_p).$$

The source strength of electrons due to galactic knock-on production is given by the following integral:

$$Q(\gamma_e,\mathbf{r}) = 1.75\rho(\mathbf{r}) 4\pi \int_{\gamma_1}^{\gamma_2} \Phi_1(\gamma_e,\gamma_p) \frac{dJ(\mathbf{r})}{d\gamma_p} d\gamma_p \quad \text{electrons/cm}^3 \text{ sec (unit}\gamma), \quad (3)$$

in which $\rho(\mathbf{r})$ is the interstellar density in g/cm^3 as a function of galactic position $\mathbf{r}$, $dJ(\mathbf{r})/d\gamma_p$ is the differential cosmic-ray proton intensity in particles/cm^2 sec sr (unitγ), and in which the limits of integration are functions of electron energy $\gamma_{1,2} = \gamma_{1,2}(\gamma_e)$.

We ignore any possible dependence on galactic position $\mathbf{r}$, and use the cosmic-ray proton spectrum discussed by Brunstein and Cline,[18] which is a smooth fit to the high-energy spectrum, summarized by Ginzburg and Syrovatskii,[22] to the intermediate energy spectrum of McDonald and Webber,[28] and to the solar

[19] S. Hayakawa and H. Okuda, Progr. Theoret. Phys. (Kyoto) **28**, 517 (1962).
[20] F. C. Jones, J. Geophys. Res. **68**, 4399 (1963).
[21] J. B. Pollack and G. G. Fazio, Phys. Rev. **131**, 2684 (1963).
[22] V. L. Ginzburg and S. I. Syrovatskii, *The Origin of Cosmic Rays* (Pergamon Press Ltd., London, 1964).
[23] R. J. Gould and G. R. Burbidge (unpublished).
[24] R. C. Hartman, P. Meyer, and R. H. Hildebrand, J. Geophys. Res. **70**, 2713 (1965).
[25] K. A. Brunstein, Phys. Rev. **137**, B757 (1965).
[26] H. J. Bhabha, Proc. Roy. Soc. (London) **A164**, 257 (1938).
[27] V. L. Ginzburg and S. I. Syrovatskii, Progr. Theoret. Phys. (Kyoto) Suppl. **20**, 1 (1961).
[28] F. B. McDonald and W. R. Webber, GSFC Contributions to the Kyoto Conference on Cosmic Rays and Earth Storm, 1961 (unpublished).

demodulated low-energy proton spectrum:

$$dJ/d\gamma_p = 1.1\gamma_p^{-2.5} \text{ protons/cm}^2 \text{ sec sr (unit}\gamma). \quad (4)$$

In order to evaluate the limits of integration in Eq. (3), we use the constraint on the cross section expressed by Eq. (2). Since the maximum possible energy is unlimited, $\gamma_2 = \infty$, while γ_1 is determined by solving the inequality $\gamma_e \leq \gamma_{\max}$ for γ_p. The result is that $\gamma_p \geq \gamma_1$, where

$$\gamma_1 = \tfrac{1}{2}s(\gamma_e-1)+\{1+\tfrac{1}{2}(1+s^2)(\gamma_e-1)+\tfrac{1}{4}s^2(\gamma_e-1)^2\}^{1/2}.$$

It can be shown that γ_1 is greater than the largest root of $\Phi_1(\gamma_e,\gamma_p)$ as a function of γ_p, which means that Φ_1 is positive throughout the range of integration. Performing the integral of Eq. (3), we obtain

$$Q(\gamma_e) = 1.75(4\pi\rho)(1.1)\left(\frac{2\pi N_0 r_e^2}{(\gamma_e-1)^2}\right)\left\{\tfrac{2}{3}\gamma_1^{-3/2}+\left[1+\frac{s^2(\gamma_e-1)^2}{2}-\frac{(1+s^2)(\gamma_e-1)}{2}\right]\right.$$
$$\times\left[-\frac{\pi}{2}-\tfrac{2}{3}\gamma_1^{-3/2}-\tfrac{1}{2}\ln\left|\frac{\gamma_1^{1/2}-1}{\gamma_1^{1/2}+1}\right|+\arctan\gamma_1^{1/2}\right]-s(\gamma_e-1)$$
$$\left.\times\left[\frac{\pi}{2}-2\gamma_1^{-1/2}-\arctan(\gamma_1^{1/2})-\tfrac{1}{2}\ln\left|\frac{\gamma_1^{1/2}-1}{\gamma_1^{1/2}+1}\right|\right]\right\} \text{electrons/cm}^3 \text{ sec (unit}\gamma), \quad (5)$$

in which s and γ_1 are given above.

Since the cross section is valid over the range $1<\gamma_e<10^6$ and the cosmic-ray spectrum (which strongly depends on the modulation model only in the region $\gamma_p<2$ where the electron production is of minor importance) is reliable over the region $\gamma_p<10^6$, the resulting source strength $Q(\gamma_e)$ is valid over that entire region of γ_e. An approximation to the expression of Eq. (5), which allows for mathematical simplifications and gives an excellent numerical fit in the $1.2<\gamma_e<10^6$ region of physical interest, is simply

$$Q(\gamma_e) = 4.9\rho(\gamma_e-1)^{-2.76} \text{ electrons/cm}^3 \text{ sec (unit}\gamma). \quad (6)$$

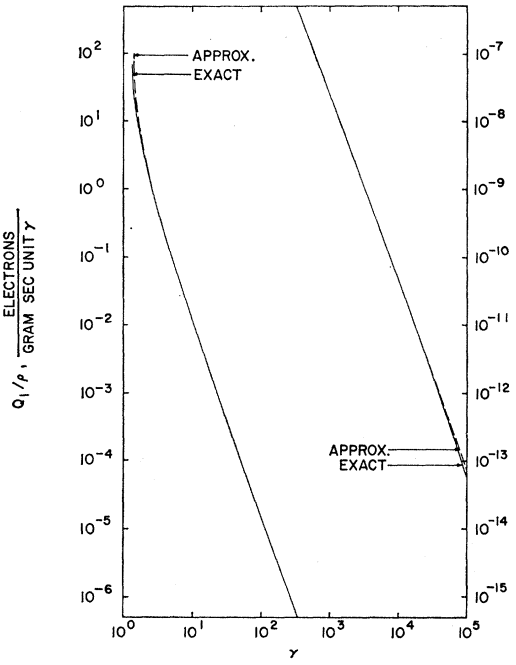

FIG. 3. The calculated source strength for galactic knock-on production per unit mass density from Eq. (5) plotted for comparison with the approximation from Eq. (6). The approximation is used in all the calculations.

Figure 3 shows the closeness of fit of the approximation to the derived expression, in which the normalized quantities $Q(\gamma_e)/\rho$ are plotted.

In order to check this result we can instead integrate the cross-section over the proton spectrum of McDonald and Webber.[28] The form they fit to the observations is $J(>R) = 0.40R^{-1.25}$ protons/cm^2 sec sr, in which the rigidity R is measured in BV. We differentiate this spectrum and change the units to obtain

$$\frac{dJ}{d\gamma_p} = \frac{dJ}{dR}\frac{dR}{d\gamma_p} = 0.54\gamma_p(\gamma_p^2-1)^{-1.625}$$
$$\text{protons/cm}^2\text{sec sr (unit}\gamma).$$

The computed source strength using this spectrum in its restricted region of validty, $2\lesssim\gamma_p\lesssim 10^2$, is nearly the same numerically as that of Eq. (6). The source strength used by Brunstein[25] for the energy interval $5<\gamma_e<50$ was $Q'(E_e) = 0.91\rho E_e^{-2.625}$ electrons/cm^3 sec MeV, which can be transformed:

$$Q'(\gamma_e) = Q'(E_e)\frac{dE}{d\gamma} = 0.91\rho(\gamma_e-1)^{-2.625}(mc^2)^{-1.625}$$
$$= 2.7\rho(\gamma_e-1)^{-2.625} \text{ electrons/cm}^3 \text{ sec (unit}\gamma).$$

This source strength, in its restricted region of validity, is also very close to that of Eq. (6).

B. Neutron-Decay Electrons

Cosmic rays produce secondary relativistic electrons also by means of nuclear reactions. In this process intermediate excited nuclei or neutrons are produced which in turn beta decay. This two-step process systematically shifts the kinetic energies involved from the BeV region to the MeV region by giving the decay electrons a distribution in energy per unit mass resembling that of the parent neutrons or excited nuclei. Since the lifetime of the neutron against decay (1000 sec) is infinitesimal compared to its lifetime against inter-

action, each secondary neutron will give rise to one secondary electron.

There are at least three sorts of cosmic-ray interactions with the interstellar medium which produce secondary neutrons. (1) π^+ mesons are produced with neutrons in the reaction $p+p\rightarrow p+n+\pi^+$. This process has the lowest energy threshold of any meson-producing reaction and excess π^+ production continues to occur in the higher energy region of multiple π^+ and π^- meson production. Except for the case of the relatively rare process $p+p\rightarrow d+\pi^+$ which competes for π^+ production, charge conservation insures that the total number of excess π^+ mesons, integrated over all energies, is equal to the number of beta-decay electrons at production. (2) Neutrons are also made by the evaporation of excited compound nuclei formed in cosmic-ray interactions. Since about 10% of interstellar material may be helium and about 15% of cosmic rays are alphas or heavier nuclei, nearly one quarter of all cosmic-ray interactions with the interstellar medium involve compound nuclei capable of excitation. Neutron emission is the most likely method of the de-excitation of compound nuclei. Although the neutrons are thermal in the reference frame of the nucleus, the cosmic-ray motion insures a spectrum up to relativistic energies in the observer's frame of reference. (3) Neutrons can also be made by a nuclear knock-on process analogous to that for atomic knock-on electrons. Neutrons made in this way have somewhat greater kinetic energies than do evaporation neutrons since less energy goes to the remaining nucleus.

The existence of these three processes requires that a secondary component of electrons should arise from nuclear reactions and also requires that this component should be characterized by energies in the MeV region. The spectrum of beta-decay electrons resulting from interstellar interactions can be reasonably estimated, but unlike that of knock-ons, cannot be calculated accurately since exact expressions for the nuclear reaction cross sections do not exist.

The probability of a neutron at rest emitting an electron within $d\gamma_1$ at γ_1 in its decay reaction $n\rightarrow e^-+p+\bar{\nu}$ is

$$f_1(\gamma_1)d\gamma_1=0.614\gamma_1(\gamma_1^2-1)^{1/2}(2.53-\gamma_1)^2d\gamma_1 \quad \text{electron/neutron}.$$

This beta-decay spectrum covers the kinetic-energy region from 0 to 782 keV, i.e., from a γ_1 of 1.0 to 2.53. The spectrum of electrons in the observer's frame, $f_3(\gamma_3)$, depends on both the spectrum of electrons relative to the parent neutrons, $f_1(\gamma_1)$, and the spectrum of neutrons relative to the observer, $f_2(\gamma_2)$. Analogous to the calculation by Jones[20] for $\pi\rightarrow\mu\rightarrow e$ electron productions, we have, for cases in which the distribution $f_3(\gamma_3)$ of electron energies in the decay frame does not depend on the spectrum $f_2(\gamma_2)$ of decay reactions relative to the observer, and for cases of isotropic collisions or decays,

$$f_3(\gamma_3)d\gamma_3=\tfrac{1}{2}d\gamma_3\int_1^{2.53}\frac{f_1(\gamma_1)d\gamma_1}{(\gamma_1^2-1)^{1/2}}\int_{\gamma_2^-}^{\gamma_2^+}\frac{f_2(\gamma_2)d\gamma_2}{(\gamma_2^2-1)^{1/2}}. \quad (7)$$

Electrons produced in $d\gamma_1$ at γ_1 are uniformly spread over the interval

$$\gamma_2\gamma_1-(\gamma_2^2-1)^{1/2}(\gamma_1^2-1)^{1/2}\leq\gamma\leq\gamma_2\gamma_1+(\gamma_2^2-1)^{1/2}(\gamma_1^2-1)^{1/2},$$

as shown by Rossi.[29] Thus, the contribution to the interval $d\gamma_3$ at γ_3 from at γ_1 is integrated over the portion of the spectrum $f_1(\gamma_1)$ which contributed to $d\gamma_3$, using the connection between γ_1 and γ_3 expressed by the limits of integration on γ_2:

$$\gamma_2^{\pm}=\gamma_1\gamma_3\pm(\gamma_1^2-1)^{1/2}(\gamma_3^2-1)^{1/2}.$$

A neutron spectrum $f_2(\gamma_2)$ can be replaced by a discrete series of intensities of monoenergetic neutrons in order to obtain a numerical result. The beta-decay spectra resulting from several monoenergetic neutron distributions are illustrated in Fig. 4. The area $\int_1^\infty f_3(\gamma_3)d\gamma_3$ under each curve is 1.

The decay spectrum of the electron is given by Eq. (5), but the neutron spectrum relative to the galactic frame $f_2(\gamma_2)$ depends, in turn, on both the neutron spectrum relative to the parent interaction, $f_4(\gamma_4)$, and the spectrum of cosmic-ray interaction, relative to the galaxy, $f_5(\gamma_5)$. The secondary-neutron spectrum, $f_4(\gamma_4)$, is a combination of at least three kinds of production spectra, as outlined earlier, and is unknown.

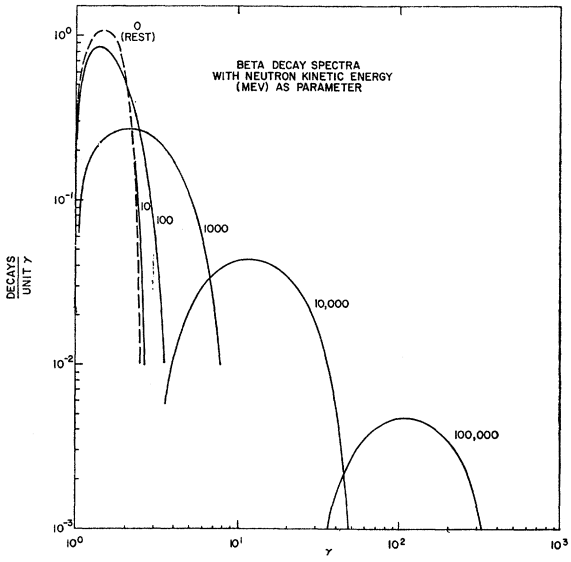

FIG. 4. Beta-decay spectra of monoenergetic neutrons. Cosmic-ray neutrons of characteristically BeV energies are seen to produce electrons having a spectrum in the MeV region; the source strength from galactic secondary neutrons is found, however, to have a significantly lower intensity than does that from knock-on production.

[29] B. Rossi, *High Energy Particles* (Prentice Hall, Inc., Englewood Cliffs, New Jersey, 1952).

However, it can be assumed that in the interaction, or center-of-momentum frame, most of the secondary neutrons have energies in the few-MeV region, low compared with BeV-like cosmic-ray energies in the galactic frame. As shown by Jones,[20] a primary power-law spectrum, when such an inequality is obeyed, produces again a power-law spectrum of secondary products with the same shape but a different normalization. In the absence of detailed knowledge of the neutron production by cosmic rays, we can therefore assume that the neutron spectrum in the galactic frame reflects the cosmic-ray spectrum with a multiplying constant containing the cross section for neutron production. We further simplify by using an energy-independent cross section of 10 mb, based on inspection of the data tabulated by Pollack and Fazio.[30] This appears to approximate the cross section for excess π^+ over π^- production, and, as discussed earlier, we can approximate by assuming that each excess π^+ is accompanied by one neutron. The source density of secondary neutron-decay electrons due to interactions of primary cosmic-ray protons is thus

$$Q_1(\gamma_3,\mathbf{r})d\gamma_3=4\pi\rho(\mathbf{r})f_3(\gamma_3)d\gamma_3 \text{ electrons/cm}^3 \text{ sec},$$

in which $f_3(\gamma_3)$ is related to $f_2(\gamma_2)$ by Eq. (7) and we approximate

$$f_2(\gamma_2)d\gamma_2\approx N_0\sigma(dJ_2/d\gamma)d\gamma_2 \text{ electrons/sec sr g}.$$

Here, $N_0=6.02\times10^{23}$ per g, $\sigma\cong1.0\times10^{-26}$ cm^2 electron/proton and $dJ_2/d\gamma_2$ is the cosmic-ray spectrum of protons/cm^2 sec sr (unitγ) given by Eq. (4). This calculated electron source strength is found to be, in the low-energy region, at least one decade below the knock-on source strength. The beta-decay source strength is thus so much less than the knock-on source density that, although its calculation is much less accurate, we assume its contribution can be neglected in the calculations that follow.

C. Galactic Energy-Loss Mechanisms

Electrons produced by the various cosmic-ray processes in the galaxy must subsequently lose energy in the galactic medium before they are observed. Since the medium is composed of matter, fields, and radiation, and has a boundary, the energy-loss mechanisms include ionization, bremsstrahlung, synchrotron radiation, inverse Compton effect, and leakage into metagalactic space. Some of these are of greater importance than others; several authors have considered these effects for the higher energy electrons from the $\pi\rightarrow\mu\rightarrow e$ process (e.g., Gould and Burbidge,[23] Ginzburg and Syrovatskii,[22] Jones,[20] Hayakawa and Okuda,[19] and others) and we review in detail the commonly used values of astrophysical parameters in order to best compare results.

Ionization loss in the interstellar medium can be taken to be energy-independent over the electron energy range of interest here; although the loss does increase slightly at the highest energies, other loss mechanisms produce a much greater effect in this higher energy region. Hayakawa and Kitao[31] have calculated the energy loss as a function of degree of ionization of the medium; if we assume the galactic medium to be mostly hydrogen and to be about 90% neutral, then we can use a value of $|dE/ds|\approx5$ MeV cm^2/g. The energy-loss rate is directly proportional to the interstellar matter density; so if we then assume a constant $\rho_{\text{halo}}=2\times10^{-26}$ g/cm^3, we can write

$$-\left(\frac{d\gamma}{dt}\right)_{\text{ion}}=\frac{c\rho}{mc^2}\left|\frac{dE}{ds}\right|=6.0\times10^{-15}\equiv k \text{ (unit}\gamma\text{)/sec}. \quad (8)$$

In the disk, the value is about 50 times as great. It is interesting to note that the *rectilinear* range in the halo of even a low-energy relativistic electron is $\approx10^{25}$ cm, much greater than the galactic diameter of 10^{23} cm; in the disk where $\rho\approx10^{-24}$ g/cm^3, it is of the same order as the diameter but much greater than the disk thickness. Whether or not electrons observed near the earth can get here from the disk or from outside the galaxy depends on considerations of propagation and of local spiral-arm trapping, which cannot be accurately depicted. It is outside the scope of this paper to attempt to take into account the spiral structure of the disk and anisotropic propagation, so we will for the most part use halo values for the galactic parameters and compare with results obtained using disk values.

Bremsstrahlung is the radiation which occurs when electrons decelerate in matter; the loss rate is proportional to the density and, using the values of the constants previously assumed, we can write

$$-\left(\frac{d\gamma}{dt}\right)_{\text{brem}}=\frac{4cr_e^2Z_T^2\rho N_0}{137A_T}\ln\left(\frac{183}{Z_T^{1/3}}\right)(\gamma-1)$$

$$\cong4.35\times10^{-18}\gamma \text{ (unit}\gamma\text{)/sec}.$$

This loss rate increases with energy, exceeding the rate due to ionization loss at energies above 700 MeV.

Synchrotron radiation, which occurs when electrons accelerate moving through magnetic fields, is an energy-loss mechanism which is independent of the matter density ρ, but depends on the square of the galactic field component $B_\perp$ perpendicular to the electron's velocity. If we assume the mean $B_\perp$ to be 3×10^{-6} G, we can write

$$-\left(\frac{d\gamma}{dt}\right)_{\text{syn}}=\frac{2cr_e^2B_\perp^2(\gamma^2-1)}{3mc^2}$$

$$\cong1.73\times10^{-20}\gamma^2 \text{ (unit}\gamma\text{)/sec}. \quad (9)$$

[30] J. B. Pollack and G. G. Fazio, Phys. Rev. **131**, 2684 (1963).

[31] S. Hayakawa and K, Kitao, Progr. Theoret. Phys. (Kyoto) **16**, 139 (1956).

In this case the rate increases by approximately the square of the energy, exceeding the rate due to ionization loss at energies above 300 MeV. Since the energy loss due to synchrotron radiation is greater than that due to bremsstrahlung at all energies for which either is more important than ionization loss, we will ignore the effects of bremsstrahlung in our calculation.

The energy loss due to *inverse Compton* collisions of electrons with interstellar photons is proportional to the radiation density and, in the region of interest here, to the square of the energy. It is usually assumed that the typical galactic halo radiation density ρ_r is approximately

$$0.1\ \text{eV/cm}^3 = 1.6\times10^{-13}\ \text{erg/cm}^3.$$

Recently, however, Penzias and Wilson[32] have detected an isotropic microwave background which is consistent with a universal blackbody distribution of radiation at a temperature of about 3°K. Dicke *et al.*[33] have postulated a primordial, cosmic fireball origin of this radiation, giving rise to a greatly red-shifted background now observable. An additional measurement[34] has supported the hypothesis further by providing a second point on a 3°K blackbody spectral fit. The additional blackbody radiation density is thus

$$\rho_b = aT^4 = \frac{8\pi^5 k^4 T^4}{15c^3h^3} \xrightarrow[T=3]{} 5.9\times10^{-13}\ \text{erg/cm}^3.$$

If we include this value, which is several times the formerly assumed halo energy density, the total energy density is now

$$\rho_t = \rho_b + \rho_r = 7.5\times10^{-13}\ \text{erg/cm}^3,$$

and we can write

$$-\left(\frac{d\gamma}{dt}\right)_{\text{comp}} = \frac{-\rho_t}{B_\perp^2/4\pi}\left(\frac{d\gamma}{dt}\right)_{\text{syn}} \cong 1.8\times10^{-20}\gamma^2(\text{unit}\gamma)/\text{sec}. \quad (10)$$

This loss rate is equal to or slightly greater than the synchrotron rate, and has the same energy dependence over all the energies of interest here, $1<\gamma\lesssim10^5$. We shall add the contributions from the two effects in the work that follows, setting $b\equiv3.5\times10^{-20}$.

The *escape* rate due to the diffusion of the electrons into metagalactic space is even less certain than the loss rates considered above, since the galactic trapping of electrons in the energy range of interest here is unknown. Electrons of these very low rigidities may be trapped in the galaxy for a time similar to the lifetime usually assumed to be representative of the high-energy cosmic-ray protons, or they may be trapped for a duration orders of magnitude longer. High-energy electrons are usually assumed to have the same mean lifetime against escape as do cosmic rays,[19,22,23] namely, $T_L=3\times10^{15}$ sec. We will leave this an open question, and assume T_L for these low energies to be energy-independent and to be between 3×10^{15} sec and ∞. For purposes of comparison, an effective energy-loss rate is taken to be the total energy of the particle divided by the lifetime:

$$-\left(\frac{d\gamma}{dt}\right)_L = \frac{\gamma}{T_L} \lesssim 3.3\times10^{-16}\gamma\ (\text{unit}\gamma)/\text{sec}.$$

The loss rate increases with energy, in the limit exceeding that rate due to ionization loss at energies above 9 MeV, and being exceeded by that due to inverse Compton and synchrotron loss above 5 BeV. Escape thus *may* dominate ionization and other losses over most of the energy range of interest in this paper, and this result is at least consistent with the use of halo-parameter values in the calculations. This process, for purposes of computation, produces a particle sink, rather than an alteration of energy, and we therefore use

$$-Q_L(\gamma) = \frac{n(\gamma)}{T_L} \lesssim 3.3\times10^{-16}\times n \equiv \lambda n\ \text{electrons/cm}^3\ \text{sec}\ (\text{unit}\gamma).$$

D. Calculation of Secondary-Galactic-Electron Intensity

The intensity of low-energy electrons produced in the galaxy by cosmic rays and subject to the energy losses outlined above is calculated by use of the continuity equation for the particle density in γ space:

$$\partial n/\partial t + \text{div}_\gamma(n\dot{\gamma}) = S.$$

Here $n(\gamma,t)d\gamma$ is the spatial density in $d\gamma$ at γ of electrons/cm^3 and $S(\gamma)d\gamma$ the source production rate of electrons/cm^3 sec. The continuity equation is rewritten then, as

$$\frac{\partial n}{\partial t} + \frac{\partial}{\partial\gamma}\left(n\sum_i \frac{d\gamma_i}{dt}\right) = \sum_i Q_i$$

in which the right-hand side is the algebraic sum of the particle sources and sinks Q_i, and

$$\frac{\partial}{\partial\gamma}\left(n\sum_i \frac{d\gamma_i}{dt}\right)d\gamma dt$$

is the net increase in the spatial density of electrons in $d\gamma$ at γ due to the various energy loss or gain mechanisms. Inserting the production and escape terms Q_i

[32] A. A. Penzias and R. W. Wilson, Astrophys. J. 142, 419 (1965).
[33] R. H. Dicke, P. J. E. Peebles, P. G. Roll, and D. T. Wilkinson, Astrophys. J. 142, 414 (1965).
[34] P. G. Roll and D. T. Wilkinson, Phys. Rev. Letters 16, 405 (1966).

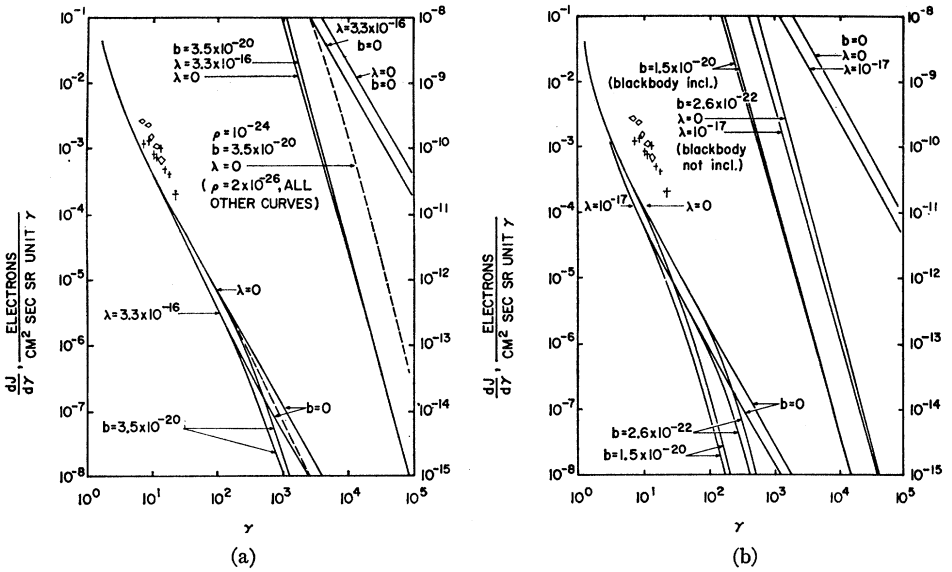

FIG. 5. (a) Calculated differential intensities of electrons produced as galactic secondaries are compared with sample observations. The results are shown with and without losses due to inverse Compton effect and synchrotron radiation and losses due to escape from the galaxy, using a halo value of the matter density. Also shown is the result in which the disk value of the density was used, and inverse Compton losses were incorporated. The higher energy intensity is higher if the disk value is used, but is still well below the observations. When no losses are used, the result is independent of the density. (b) Upper limits to the calculated differential intensities of electrons from metagalactic secondary production. Again, inverse Compton and synchrotron losses and red-shift escape losses are varied for comparison, and, in this case, results are plotted with and without blackbody radiation. In all cases, the calculated metaglactic intensities are below the galactic intensities.

and the energy-loss terms $d\gamma_i/dt$ discussed earlier, we have

$$\frac{\partial n}{\partial t}-(k+b\gamma^2)\frac{\partial n}{\partial \gamma}+(\lambda-2b\gamma)n=Q_1(\gamma), \qquad (11)$$

in which k, b, and λ represent the positive numerical coefficients outlined above for ionization loss, inverse-Compton and synchrotron losses, and escape, respectively, and Q_1 refers to the knock-on source strength. The solution to this equation for $n(\gamma)$ is shown in the Appendix to have various forms, depending on which various energy-loss mechanisms are taken to be dominant. Since knowledge of the astrophysical parameters is uncertain, we exhibit here all the solutions.

First, in the limiting case at the lowest energies when only ionization losses and escape losses are relevant,

$$n_e(\gamma)|_{b=0}=\frac{e^{\lambda\gamma/k}}{k}\int_\gamma^{\gamma+tk}Q(\gamma')e^{-\lambda\gamma'/k}d\gamma'$$

electrons/cm³ (unitγ).

If we use for $Q(\gamma')$ the knock-on source expression of Eq. (6), and take $t\rightarrow\infty$, the integral can be analytically evaluated for $\lambda\rightarrow 0$, and can be numerically evaluated for finite λ. The resulting differential intensities,

$$dj_e/d\gamma=cn/4\pi \text{ electrons/cm}^2 \text{ sec sr (unit}\gamma),$$

are plotted in Fig. 5.

Second, in the much higher energy region when inverse-Compton and synchrotron losses predominate,

$$\frac{dj_e}{d\gamma}=\frac{ce^{f(k,\lambda,b,\gamma)}}{4\pi(k+b\gamma^2)}\int_\gamma^\infty Q(\gamma')e^{-f(k,\lambda,b,\gamma')}d\gamma'$$

electrons/cm² sec sr (unitγ),

in which

$$f(k,\lambda,b,\gamma)=\frac{\lambda}{(kb)^{1/2}}\arctan\frac{b^{1/2}\gamma}{k^{1/2}}.$$

In the event of no escape losses, we have

$$\left.\frac{dj_e}{d\gamma}\right|_{\lambda=0}=\frac{c}{4\pi(k+b\gamma^2)}\int_\gamma^\infty Q(\gamma')d\gamma'.$$

These calculated intensities are also plotted in Fig. 5. Comparison of the calculated secondary intensities with the intensity observed by Cline *et al.*[5] shows that the calculated absolute intensity is too low. Further, using the modulation model of Parker,[7] the interstellar value would be a factor of 2.7 higher than the value observed, increasing the discrepancy. We claim that this discrepancy is not trivial; i.e., the lack of knowledge of astrophysical parameters is not a contributing factor in this lack of fit. In the limiting low-energy case in which only ionization losses contribute, the secondary electrons are in an equilibrium state such that the matter density cancels out:

$$\left.\frac{dj_e}{d\gamma}\right|_{b=0\lambda=0}=\frac{c}{4\pi k}\int_\gamma^\infty Q(\gamma')d\gamma'=\frac{c}{4\pi k}\left(\frac{4.9\rho}{1.76(\gamma-1)^{1.76}}\right)$$

electrons/cm² sec sr (unitγ), in which k is directly proportional to ρ. Thus, since the ionization losses and knock-on cross section are well known, the calculated intensity *in this case* requires only the assumption of a constant intensity of cosmic rays throughout the region where the observed secondary electrons are produced. In this limiting case, then, considerations of the spiral galactic structure and of the gas densities in the propagation media of the halo and disk become unimportant.

III. SECONDARY METAGALACTIC ELECTRONS

A. Production Mechanisms

Secondary electrons can be made in metagalactic space by cosmic-ray interactions with that medium. Although the character of the intergalactic cosmic-ray intensity and of the medium are poorly known, we can still expect that the secondary low-energy electrons will be in an equilibrium similar to that in the galaxy. As was seen in the previous section, the fundamental quantity needed in order to calculate the secondaries is the primary cosmic-ray intensity. Some theorists assume that the metagalactic intensity is about the same as that observed in the galaxy; for purposes of calculation we will take it to be an upper limit.

Although the degree of ionization of the intergalactic medium is uncertain, we can make the usual assumption that it is essentially totally ionized; the cross section for knock-on production by Coulomb collisions with free plasma electrons is essentially the same as that for bound electrons. Nuclear interactions of cosmic rays with free protons will produce neutron-decay electrons as well, but again to a lesser extent; in fact, evaporation neutron production will be even less competitive in intergalactic space if we assume that both the cosmic rays and the medium contain negligible portions of alpha particles.

We then take the metagalactic secondary source strength to be given by

$$Q_m(\gamma_e) \lesssim \frac{4.9}{1.75}\rho(\gamma_e-1)^{-2.76} \approx 2.8\rho(\gamma_e-1)^{-2.76} \text{ electrons/cm}^3 \text{ sec (unit}\gamma),$$

in which ρ is the density in g/cm³. This source strength does not directly include an estimate of the number of electrons that leak from galaxies into the intergalactic medium; however, the primary cosmic-ray intensity responsible for it is taken, as an upper limit, to be the same as in the galaxy, so that in the low-energy equilibrium region a source strength approximately equal to that leakage rate is implied.

B. Metagalactic Energy-Loss Mechanisms

Secondary electrons produced in intergalactic space lose energy through their interaction with that medium, and also vanish because of the Hubble expansion. Assuming knowledge of the physical parameters involved, these losses can be calculated. In addition, there may be a distortion of the energy spectrum due to the effects of the penetration into the galaxy, just as there is into the interplanetary region.

Ionization losses in a fully ionized medium are replaced by losses due to plasma oscillations; the cosmic-ray electron loses energy by interacting with the plasma ions and electrons to a greater extent than it would in a neutral medium since the shielding of the individual charges is reduced. As shown by Hayakawa and Kitao,[31] for an ionized medium we have

$$|dE/ds|_{\text{mg}} = 10 \text{ MeV cm}^2/\text{g}.$$

If we assume a universal proton density of 10^{-5}/cm³, or an equivalent matter density $\rho_{\text{mg}} = 1.6\times10^{-29}$ g/cm³, using Eq. (8) we have for the energy-loss rate

$$-(d\gamma_e/dt)_{\text{ion}} = 1.0\times10^{-17} \text{ (unit}\gamma)/\text{sec}.$$

It is interesting to note that the rectilinear range of a low-energy relativistic electron is about 10^{28} cm, close to the Hubble radius. Thus, electrons produced universally can reach the galaxy. The ratio of metagalactic to galactic bremsstrahlung losses is the same as that ratio for "ionization" losses. This is because both interactions depend linearly on the matter density, and because a factor of 2 is introduced in each loss when one substitutes an ionized medium for a nearly neutral one. Thus,

$$-(d\gamma_e/dt)_{\text{brem}} \cong 7.0\times10^{-21}\,\gamma_e \text{ (unit}\gamma)/\text{sec}.$$

The bremsstrahlung loss equals that due to plasma excitation at $\gamma_e = 1.4\times10^3$ or about 700 MeV.

Synchrotron and inverse-Compton losses depend on the typical metagalactic magnetic-field strength and photon density, which are unknown but have usually been assumed to be about 10^{-7} G, and 6.0×10^{-3} eV/cm³ $\approx 10^{-14}$ erg/cm³, respectively. If we add the universal blackbody radiation density 5.9×10^{-13} erg/cm³, we have from Eqs. (9) and (10)

$$-(d\gamma_e/dt)_{\text{syn}} \cong 2.0\times10^{-23}\gamma^2 \text{ (unit}\gamma)/\text{sec}$$

and

$$-(d\gamma_e/dt)_{\text{comp}} \cong 1.5\times10^{-20}\gamma^2 \text{ (unit}\gamma)/\text{sec, including blackbody radiation}$$

$$\cong 2.4\times10^{-22}\gamma^2 \text{ (unit}\gamma)/\text{sec, not including blackbody radiation}.$$

Inverse-Compton losses in either case thus dominate synchrotron losses at all energies. The plasma-excitation losses dominate inverse-Compton losses for all energies up to 13 MeV, or up to 100 MeV, depending on whether we include the effect due to a supposedly universal blackbody radiation. In either case synchrotron and bremsstrahlung losses are dominated, and Compton effect is the only high-energy loss mechanism we will consider.

The magnitude of the effective particle sink represented by universal expansion, the red-shift loss, is uncertain since the diffusion of electrons in intergalactic space cannot be accurately represented. We will, therefore, in analogy to the galactic case, take as an upper limit the rectilinear loss due to the three-dimensional expansion, characterized by a lifetime one-third the Hubble factor: $T_L=\frac{1}{3}H$. The equivalent energy loss rate is

$$-\left(\frac{d\gamma_e}{dt}\right)_L\leq\frac{\gamma}{T_L}\leq 1.0\times10^{-17}\gamma\ (\text{unit}\gamma)/\text{sec}.$$

This loss rate is exceeded by that due to inverse Compton effect above *about* 300 MeV, if we include the *blackbody* radiation, and if not, above 20 BeV, but it actually exceeds that due to plasma excitation at all energies above $\gamma=1$. For our computation we represent this process as a sink of particles and so

$$-Q_L(\gamma)=n(\gamma)/T_L\leq 1.0\times10^{-17}\times n$$
$$\text{electrons/cm}^3\ \text{sec}\ (\text{unit}\gamma).$$

C. Calculation of Secondary-Metagalactic-Electron Intensity

The intensity of low-energy electrons produced in intergalactic space by cosmic rays with an assumed universal intensity is calculated by use of the equations derived earlier. Using the values stated above for intergalactic plasma-excitation and inverse-Compton losses, we solve for two extreme cases, namely, that for the rectilinear red-shift loss and that for none. These are plotted in Fig. 5. It is seen that the metagalactic flux, even for a primary cosmic-ray flux equal to that observed here, is at least an order of magnitude below the calculated galactic electron flux. The analogous result for the high-energy secondaries was obtained by Gould and Burbidge.[23] Thus, since this calculated metagalactic-electron intensity is an upper limit, it represents a negligible addition to the galactic secondary flux, and we must look elsewhere for a possible source for the experimentally observed electrons.

IV. ENERGY INPUTS TO SECONDARY ELECTRONS

In this section we consider the possibility that the observed low-energy electrons are galactic secondaries which have been accelerated after their creation. Two mechanisms for increasing the electron intensity to that observed present themselves, one in the solar system producing a local intensity increase, and the other producing an intensity increase throughout interstellar space.

A. Heliocentric Electric Field

The possibility of the presence of a substantial potential of the solar system with respect to the galaxy as a whole has been considered by several authors. In particular, attempts have been made to explain the solar modulating effects of primary cosmic rays in terms of such a potential. Earlier work by Ehmert[35] required a positive potential of 1 or more BV to account for the observed modulation. A more recent treatment by Freier and Waddington[36] required 50 MV to obtain quantitative agreement between their model and the observed spectrum. It is nevertheless difficult to envision how even such a modest electric field could be maintained in the presence of the interstellar gas which is, undoubtedly, somewhat ionized.

In this section we consider the effects of such a heliocentric electric field on the interstellar secondary electrons, which we have shown must be produced with an intensity not far from that observed.

The Liouville theorem states that the differential density of electrons

$$\frac{dN}{(4\pi r^2dr)(4\pi p^2dp)}$$

remains constant along trajectories in phase space. From this, we find that

$$(dJ/d\gamma)(1/p^2)$$

is a constant. Relating the spectrum outside the solar system, $dJ_1/d\gamma$, to that observed, $dJ_2/d\gamma$, we have

$$\frac{dJ_2}{d\gamma}\{(\gamma mc^2+qV)^2-(mc^2)^2\}^{-1}=\frac{dJ_1}{d\gamma}\{(\gamma mc^2)^2-(mc^2)^2\}^{-1},$$

where qV is the product of the charge on the electrons and the accelerating potential. Relating the measured intensity, defined here as

$$\frac{dJ_2}{d\gamma}=\frac{dJ}{d\gamma}(\gamma mc^2+qV)$$

to the calculated secondary intensity,

$$\frac{dJ_1}{d\gamma}=\frac{dJ}{d\gamma}(\gamma mc^2),$$

we find that a potential of 1.5 MV provides an excellent fit to the data at the low energies. This result is shown in Fig. 6.

The intensity increase provided by this 1.5-MV field is insufficient to simultaneously fit the observations at the high energies. The negative electrons in the fractional-BeV energy region, found to be in excess of those from $\pi\rightarrow\mu\rightarrow e$ decay by DeShong, Hildebrand, and Meyer,[3] would thus have to be due to yet another source. Such may or may not be the case, but a third

[35] A. Ehmert, in *Proceedings of the Cosmic Ray Conference, 1959* (Academy of Sciences of the U.S.S.R., Moscow, 1960), Vol. IV, p. 142.

[36] P. S. Freier and C. J. Waddington, Space Sci. Rev. 4, 313 (1965).

source is undesirable from the point of view of minimizing hypotheses. The observations may yet indicate that there could be a change in the spectral form between 20 and 200 MeV, but it will have to be determined whether this is due to solar modulation. If we assume that there is only one electron source other than the $\pi \rightarrow \mu \rightarrow e$ process, we thus need to look elsewhere for the required energy input. Further, a 50-MV field would so grossly distort the 3-MeV electron spectrum from galactic knock-on production as to be experimentally evident from a vast oversupply of low-energy electrons. We conclude that a heliocentric field hypothesis is not a likely candidate as the source of the observed low-energy electrons.

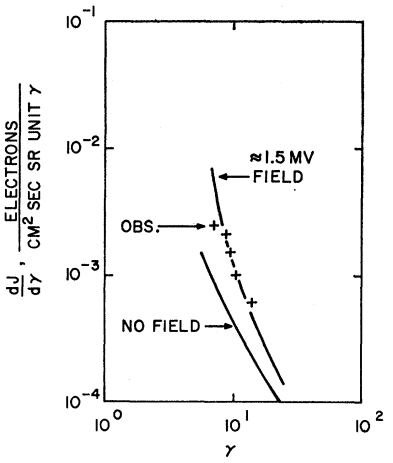

FIG. 6. Calculated differential intensity of electrons resulting from galactic knock-on production and accelerated by a heliocentric field of 1.5 MV. If such a field exists, the low-energy observations can be accounted for, but the high-energy electrons remain in excess of secondary meson production.

B. Galactic Fermi Acceleration

The acceleration mechanism of cosmic-ray protons most generally considered as a possible means of *interstellar* energy increase is the mechanism first investigated by Fermi.[6] In this model, a particle randomly gains energy in the process of colliding with moving magnetic irregularities in the medium in which it is confined. The probability for it to have total energy between γ and $\gamma+d\gamma$ is

$$\frac{d\pi}{d\gamma}(\gamma)d\gamma=\frac{1}{T\alpha}\frac{\gamma_0^{1/T\alpha}}{\gamma^{1+1/T\alpha}}d\gamma,$$

in which γ_0 is the particle's value at injection, T is the mean life of the particles, and $\alpha\equiv v^2/(c^2\tau)$, in which v is the scattering-center velocity, and τ is the mean time between collisions. Thus,

$$\frac{dJ}{d\gamma}=\frac{J_0}{T\alpha}\frac{\gamma_0^{1/T\alpha}}{\gamma^{1+1/T\alpha}},$$

in which

$$J_0\equiv\int_1^\infty\frac{dJ}{d\gamma}d\gamma,$$

showing that the resultant cosmic-ray spectrum should obey a power law in total energy. Since this result is, in fact, consistent with observations, a mechanism of the Fermi type gains much support, whether operative in the interstellar medium, or in stellar atmospheres, or in supernovae.

If we now investigate the possibility that electrons may also be Fermi-accelerated, we treat the mechanism as an energy input in the solution of the continuity equation for electrons in energy space. Since, in the Fermi model, the energy acquired by a particle of age t is $\gamma=\gamma_0e^{\alpha t}$ in which α is defined above, we have

$$+(d\gamma/dt)_{\text{Fermi}}=\alpha\times\gamma\ (\text{unit}\gamma)/\text{sec}.$$

Inserting this term in the continuity equation, we have

$$\frac{\partial n}{dt}-(k-\alpha\gamma+b\gamma^2)\frac{\partial n}{d\gamma}+(\alpha+2b\gamma+\lambda)n=Q(\gamma) \quad (12)$$

in place of Eq. (11). Since there now exist both positive and negative energy-loss terms, the solutions to this equation do not directly follow from those used earlier. As shown in the Appendix, the forms of the solutions vary, depending on the choice of the parameters k, α, b, and λ. In particular, the algebraic sign of $(\alpha^2-4kb)\equiv\nu^2$ is the determining factor; i.e., whether α is greater or smaller than about 2×10^{-17} sec^{-1}, using a halo density of 2×10^{-26} g cm^{-3}. As we shall see, any value of α that comes close to giving a fit to the experimental data is much greater than this; so we can, except for the postulated $\alpha\equiv0$ case discussed earlier, take (γ^2-4kb) to be positive.

As discussed in the Appendix, care must be taken that the behavior is correctly interpreted near the singularities which occur at energies

$$\gamma^{\pm}\equiv\tfrac{1}{2}b\{\alpha\pm(\alpha^2-4kb)^{1/2}\},$$

where the rate of energy loss changes signs. The solutions for

$$dj_e/d\gamma=cn_e/4\pi$$

are described for the various cases of escape and synchrotron losses being or not being incorporated. For $\gamma<\gamma^+$, which we shall see is the energy range of interest here, the general solution is

$$\frac{dj_e}{d\gamma}=\frac{c}{4\pi(k-\alpha\gamma+b\gamma^2)}\left(\frac{\gamma^+-\gamma}{\gamma-\gamma^-}\right)^{\lambda/\nu}\times\int_\gamma^{\gamma^-}Q(\gamma')\left(\frac{\gamma'-\gamma^-}{\gamma^+-\gamma'}\right)^{\lambda/\nu}d\gamma'.$$

Its limiting form for $\lambda\rightarrow0$ follows directly, but for $b\rightarrow0$ it is more convenient to solve the original differential equation to yield

$$\left.\frac{dj_e}{d\lambda}\right|_{b=0}=\frac{c}{4\pi k(1-\alpha\gamma/k)^{1+\lambda/\alpha}}\int_\gamma^{k/\alpha}Q(\gamma')\times(1-\alpha\gamma'/k)^{\lambda/\alpha}d\gamma',$$

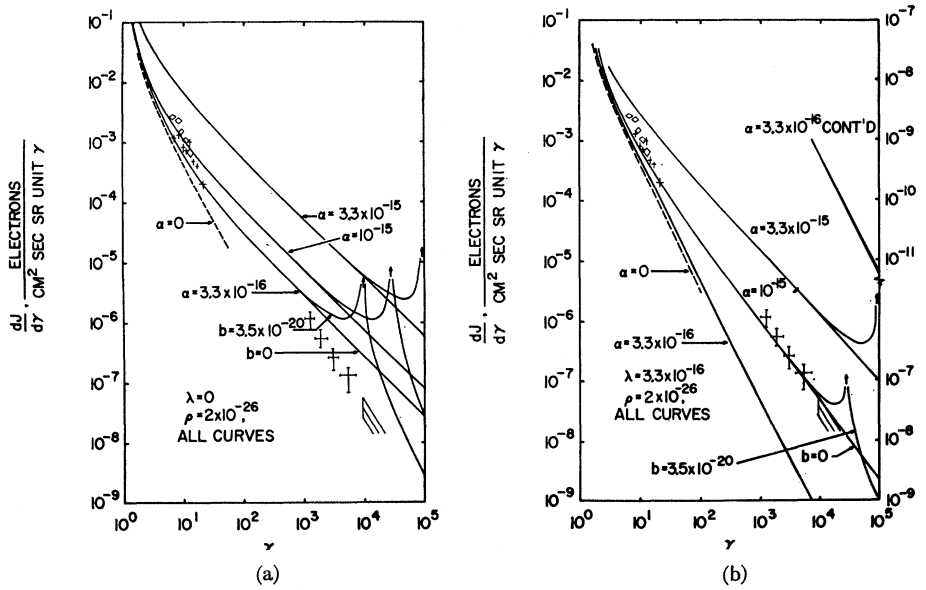

FIG. 7. Calculated differential intensities of secondary electrons which have been accelerated by a galactic Fermi process. Various values of γ are incorporated for which the results are plotted in (a) without, and in (b) with, escape losses. The galactic-halo value of the matter density is used through- It is seen that the observations, samples of which are shown, can be roughly fitted with a sufficiently large value of α. (A smaller α provides a high-energy fit if the disk density value were used, but a simultaneous fit to the low-energy intensity is not possible.) For certain combinations of the galactic parameters ρ, b, λ, and α, peaks in the intensity occur at normalized energies equal to k/α.

which also has an evident limit for $\lambda \to 0$. These results are plotted in Fig. 7 for various values of α. If α is large enough it is possible to match the intensity but a poor fit to the spectral shape is obtained.

If one attributes the primary proton beam to Fermi acceleration and the further assumption is made that the parameters α and λ are nearly the same for protons and electrons, as shown by Fermi[6] we have for the proton beam

$$dJ/d\gamma = \text{const} \times \gamma^{-(1+\lambda/\alpha)}.$$

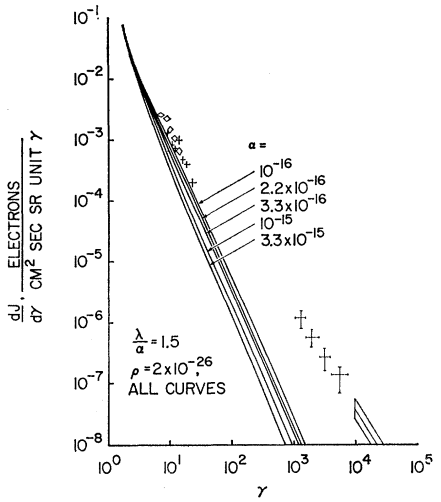

FIG. 8. Calculated differential intensities of secondaries for a fixed ratio of $\lambda/\alpha = 1.5$. Here the singularity disappears at the high energies, but the low-energy fit becomes independent of λ and α and is seen to be inadequate to account for the observations.

The exponent $(1+\lambda/\alpha)$ is well established to be approximately 2.5. We now must have $\lambda > \alpha$ instead of $\lambda \lesssim \alpha$. Here $\lambda = 1.5\alpha$, and the singularity in the differential electron spectrum is removed. This solution is shown in Fig. 8 for a variety of values of λ and α, including those used formerly. In this case, toward the lower energies the resulting spectrum becomes independent of λ and α and has the same slope as the observed spectrum, but, like the solution for $\alpha = 0$ which it approaches, is too low in intensity. It appears that if the electrons are propagated similarly to the protons, such that a Fermi acceleration with $\lambda/\alpha = 1.5$ is present, the secondaries from interstellar knock-on production cannot account for the observations. Of course, it is not obvious that either λ or α would have the same values for electrons as they have for protons, or that λ/α must necessarily be equal to 1.5. The electrons have a much lower rigidity than the protons do at a given γ; they would therefore have a greater lifetime against escape and possibly a much different acceleration.

We can conclude that both the intensity and the shape of the observed low-energy electron spectrum cannot simultaneously be accounted for by galactic knock-on secondaries.

V. CONCLUSION

The secondary electron spectrum to be expected from $\pi \to \mu \to e$ decay as calculated by Hayakawa and Okuda,[19] Jones,[20] and others, coupled with the positron-electron measurements by DeShong *et al.*[3] and by Hartman *et al.*,[12] indicate that meson-decay electrons

cannot adequately explain the observed properties of high-energy cosmic-ray electrons.

Two of the authors have in a previous paper[18] discussed the possibility that the electrons may be of a primary nature, being accelerated in the same process along with cosmic-ray protons. We have here examined the possibility that cosmic-ray electrons are secondary to the nuclear beam, arising from both knock-on collisions and from the beta decay of the resultant neutrons from nuclear interactions in the interstellar gas and in metagalactic space. We conclude that neutron-decay electrons are well below the intensity to be expected from knock-on collisions and thus may be neglected as a potential source. However, at least at low energies, an accurate calculation of the knock-on electron intensity shows it to be well above that expected from $\pi \rightarrow \mu \rightarrow e$ decay but substantially below the measured intensity of low-energy electrons.

We have therefore postulated two prospective models to account for the observed electrons as being due to these knock-on electrons: (1) the knock-on electrons are further accelerated after their injection by a heliocentric electric field, (2) the knock-on electrons are accelerated after injection by a general galactic Fermi mechanism.

The first possibility, the heliocentric electric field, requires only a modest 1.5 MV to boost the calculated knock-ons to the observations; however, it does not appreciably affect the higher energy electrons where we still must face the question of the excessive negative electrons. Moreover, it is difficult to envision how even a modest potential of 1.5 MV could be maintained by the solar system (Lam and Sandri[37]).

The second possibility, that of Fermi acceleration after *secondary* production, is seen to have limitations. The value of the parameter α, defined by $+(d\gamma/dt)\equiv\alpha\gamma$, is varied in the neighborhood of that value which produces an approximate fit to the data, $\alpha\approx 10^{-15}$ sec^{-1}. When a lifetime against escape of about 10^8 yr is assumed ($\lambda\equiv 3.3\times 10^{-16}$ sec^{-1}) the observed intensity can be roughly fitted, although the fit to the slope in the low-energy region is poor. In the high-energy region, if we assume that about half of the electrons are accounted for by $\pi \rightarrow \mu \rightarrow e$ decay, we find that the remainder can also be roughly fitted. However, in this case, the value of α is quite large, $>10^{-15}$ sec^{-1}, and is about the same as that value shown by Brunstein and Cline[18] to describe the electron intensity in terms of Fermi-accelerated *primary* thermal electrons. If these parameters accurately represent galactic conditions, then we may draw the conclusion that the cosmic-ray beam will be composed of both secondary knock-on electrons and primary electrons Fermi-accelerated in essentially equivalent fractions. If the actual value of the parameter α is smaller, the secondary electrons account for a smaller fraction of the observed intensity. On the other hand, if the value of the ratio λ/α is a constant 1.5, as is usually assumed for protons, then in the low-energy region fitting a calculation of secondary electrons alone to the observations is impossible.

We can conclude, in any case, that the secondary hypothesis alone cannot account for the observations and that at least half of the observed low-energy electrons have a primary origin. We note that the observations of the charge ratio led to a similar conclusion for the high-energy electrons.[3,12] We feel, therefore, that a primary cosmic-ray beam of electrons is present throughout the energy region $\gamma\gtrsim 1$ to $\gamma>10^5$, having about the same velocity spectrum as the cosmic-ray protons in the $1<\gamma<10^2$ region. However, further observations in the $\gamma<5$ and $\gamma>10^5$ regions are desirable to better understand the properties of these primaries, and more details in the $20<\gamma<200$ region are desirable to map the transition between the knock-on and the $\pi \rightarrow \mu \rightarrow e$ secondary contributions.

APPENDIX

The equation to be solved is

$$\frac{\partial n}{\partial t}-(k-\alpha\gamma+b\gamma^2)\frac{\partial n}{\partial \gamma}+(\alpha-2b\gamma+\lambda)n=Q(\gamma), \quad \text{(A1)}$$

in which $n=n(\gamma,t)$. The initial condition assumed is $n(\gamma,t=0)=0$, and the solution is obtained by the method of characteristics.

Before proceeding to the actual solution we consider two possibilities:

(1) Particles produced with certain energies lose some of their energy when propagating through the medium, while others, produced with energies in a different range, gain energy from the medium. This implies that $d\gamma/dt$ changes sign, and for this to be so it is necessary that

$$\nu^2\equiv\alpha^2-4kb \quad \text{(A2)}$$

be greater than zero. The changes in sign occur at the energies

$$\gamma^{\pm}=(\alpha\pm\nu)/2b. \quad \text{(A3)}$$

When $4kb/\alpha^2\ll 1$, we have the approximations

$$\left.\begin{matrix}\gamma^+\approx\alpha/b\\ \gamma^-\approx k/\alpha\end{matrix}\right\}.$$

(2) Particles produced with any energy never gain energy from the medium. This implies that for all energies $d\gamma/dt<0$, and hence that

$$\mu^2\equiv 4kb-\alpha^2 \quad \text{(A4)}$$

be greater than zero.

We treat these two cases separately.

[37] H. Lam and G. Sandri (private communication).

Predominance of Energy Increase

Here $\alpha^2-4kb>0$.

The solution for this case is

$$n(\gamma,t)=\frac{(\gamma-\gamma^+)^{\lambda/\nu-1}}{(\gamma-\gamma^-)^{\lambda/\nu+1}}\int_\gamma^{g(\gamma,t)} Q(\gamma')\left(\frac{\gamma'-\gamma^-}{\gamma'-\gamma^+}\right)^{\lambda/\nu} d\gamma', \quad \text{(A5)}$$

where

$$g(\gamma,t)\equiv\frac{\gamma^+(\gamma-\gamma^-)e^{-\nu t}-\gamma^-(\gamma-\gamma^-)}{(\gamma-\gamma^-)e^{-\nu t}}. \quad \text{(A6)}$$

At this stage we want to investigate the behavior of $n(\gamma,t)$ at the exceptional points $\gamma=\gamma^\pm$. One finds, by using the L'Hospital's rule and the form (A6) of $g(\gamma,t)$, that

$$\lim_{\gamma\to\gamma^-} n(\gamma,t)=\frac{Q(\gamma^-)}{\lambda+\nu}(1-e^{-(\lambda+\nu)t}). \quad \text{(A7)}$$

Therefore at $\gamma=\gamma^-$, there is no singularity in $n(\gamma,t)$ for all times.

To find the limiting value of $n(\gamma,t)$ when $\gamma\to\gamma^+$, it is necessary to go to the original Eq. (1) and proceed there to the limit, since precisely at this energy there is a singularity also in the integrand of (A5) in addition to the one outside the integral. Finally we obtain

$$\lim_{\gamma\to\gamma^+} n(\gamma,t)=\frac{Q(\gamma^+)}{\lambda-\nu}(1-e^{-(\lambda-\nu)t}). \quad \text{(A8)}$$

Equation (A8) shows that two possibilities may arise:

(i) $\lambda-\nu>0$:

Here there is no singularity at $\gamma=\gamma^+$ for all times, and

$$n(\gamma^+,t=\infty)=Q(\gamma^+)/(\lambda-\nu). \quad \text{(A9)}$$

(ii) $\lambda-\nu\leq 0$:

Here there is no singularity for finite times but when $t\to\infty$, then

$$n(\gamma^+,t=\infty)=\infty. \quad \text{(A10)}$$

This situation persists when $\lambda\to 0$.

In order to determine, [for case (ii)], the behavior of $n(\gamma,t)$ when a steady state prevails, we must investigate the rate of energy loss,

$$d\gamma/dt=-(k-\alpha\gamma+b\gamma^2) \quad \text{(A11)}$$

and find the time intervals needed by particles produced at certain energies to achieve different energies. One finds that all $\gamma<\gamma^+$, a steady state will be reached when $t\to\infty$; while for $\gamma>\gamma^+$, the steady state is attained after a finite time interval $t_{\max}$ given by

$$t_{\max}=-\int_\gamma^\infty \frac{d\gamma'}{k-\alpha\gamma'+b(\gamma')^2}=\frac{1}{\nu}\ln\frac{\gamma-\gamma^-}{\gamma-\gamma^+}. \quad \text{(A12)}$$

One finds that when $t\to\infty$, $f(\gamma,t)\to\gamma^-$; and when $t\to t_{\max}$, $f(\gamma,t)\to\infty$. Therefore the steady-state solution $n_s(\gamma)$ is

$$n_s(\gamma)=\frac{1}{k-\alpha\gamma+b\gamma^2}\left(\frac{\gamma^+-\gamma}{\gamma-\gamma^-}\right)^{\lambda/\nu}\int_\gamma^{\gamma^-} Q(\gamma')\times\left(\frac{\gamma'-\gamma^-}{\gamma^+-\gamma'}\right)^{\lambda/\nu} d\gamma', \quad \text{for } \gamma<\gamma^+,$$

and

$$=\frac{1}{k-\alpha\gamma+b\gamma^2}\left(\frac{\gamma-\gamma^+}{\gamma-\gamma^-}\right)^{\lambda/\nu}\int_\gamma^{\infty} Q(\gamma')\times\left(\frac{\gamma'-\gamma^-}{\gamma'-\gamma^+}\right)^{\lambda/\nu} d\gamma', \quad \text{for } \gamma>\gamma^+. \quad \text{(A13)}$$

Note that for $\lambda>\nu$, $n_s(\gamma)$ has no singularities; while for $\lambda\leq\nu$, the only singularity is located at $\gamma=\gamma^+$, corresponding to a pileup of particles on the energy axis where synchrotron loss equals Fermi-acceleration gain.

The integral appearing in (A13) cannot be evaluated in closed form for arbitrary values of λ/ν. For the special case $\lambda\to 0$ we have

$$\lim_{\lambda\to 0} n_s(\gamma)\equiv n_s(\gamma)=\frac{1}{k-\alpha\gamma+b\gamma^2}\int_\gamma^{\gamma'\approx k/\alpha} Q(\gamma')d\gamma', \quad \text{for } \gamma<\gamma^+$$

$$=\frac{1}{k-\alpha\gamma+b\gamma^2}\int_\gamma^{\infty} Q(\gamma')d\gamma', \quad \text{for } \gamma>\gamma^+. \quad \text{(A14)}$$

If $b=0$, the equation for $n(\gamma,t)$ is

$$\frac{\partial n}{\partial t}-(k-\alpha\gamma)\frac{\partial n}{\partial\gamma}+(\alpha+\lambda)n=Q(\gamma) \quad \text{(A15)}$$

and the solution is

$$n(\gamma,t)=\frac{1}{k(1-\alpha\gamma/k)^{1+\lambda/\alpha}}\int_\gamma^{f(\gamma,t)} Q(\gamma')\times\left(1-\frac{\alpha\gamma'}{k}\right)^{\lambda/\alpha} d\gamma', \quad \text{(A16)}$$

where

$$f(\gamma,t)\equiv\frac{k-(k-\alpha\gamma)e^{-\alpha t}}{\alpha}. \quad \text{(A17)}$$

There is no singularity; in fact at the point

$$\gamma=k/\alpha\equiv\gamma_0$$

we obtain

$$\lim_{\gamma\to\gamma_0} n(\gamma,t)=\frac{1}{\alpha+\lambda}Q(\gamma_0)(1-e^{-\alpha t}). \quad \text{(A18)}$$

The steady-state solution is obtained when we let $t\to\infty$:

$$n_s(\gamma)=\frac{1}{k(1-\alpha\gamma/k)^{1+\lambda/\alpha}}\int_{\gamma}^{\gamma_0\equiv k/\alpha} Q(\gamma')\times\left(1-\frac{\alpha\gamma'}{k}\right)^{\lambda/\alpha}d\gamma' \quad \text{(A19)}$$

for $\gamma<\gamma_0$, and

$$n_s(\gamma)=\frac{1}{k(\alpha\gamma/k-1)^{1+\lambda/\alpha}}\int_{\gamma_0\equiv k/\alpha}^{\gamma} Q(\gamma')\left(\frac{\alpha\gamma'}{k}-1\right)^{\lambda/\alpha}d\gamma'$$

for $\gamma>\gamma_0$.

For $\lambda\to 0$ (or $\lambda\ll\alpha$), the steady-state solution is

$$n_s(\gamma)=\frac{1}{k-\alpha\gamma}\int_{\gamma}^{k/\alpha} Q(\gamma')d\gamma', \quad \text{(A20)}$$

which is the special case evaluated by Brunstein.[25]

Predominance of Energy Decrease

Here $\mu^2\equiv 4kb-\alpha^2>0$.

The solution for this case is

$$n(\gamma,t)=\frac{1}{k-\alpha\gamma+b\gamma^2}\exp\left(\frac{2\mu}{\lambda}\arctan\frac{2b\gamma-\alpha}{\mu}\right)\int_{\gamma}^{h(\gamma,t)} Q(\gamma')\times\exp\left(\frac{-2\lambda}{\mu}\arctan\frac{2b\gamma'-\alpha}{\mu}\right)d\gamma', \quad \text{(A21)}$$

where

$$h(\gamma,t)=\frac{\alpha}{2b}-\left(\frac{\mu}{2b}\right)\frac{\alpha-2b\gamma-\mu\tan(\mu t/2)}{\mu+(\alpha-2b\gamma)\tan(\mu t/2)}. \quad \text{(A22)}$$

Equation (A21) implies an electron density *periodic* in time, a result which obviously is inadmissible if not interpreted correctly. We show that beyond a certain characteristic time $t_{\max}$ the expression (A21) for $n(\gamma,t)$ loses all meaning. This follows immediately from Eq. (A11), when we note that for the case under consideration

$$\frac{d\gamma}{dt}=-b\left\{\left(\gamma-\frac{\alpha}{2b}\right)^2+\left(\frac{\mu}{2b}\right)^2\right\}<0. \quad \text{(A23)}$$

The particles therefore always decelerate. We define $t_{\max}$ as the time needed for a particle of infinite initial energy to decelerate to energy γ:

$$-t_{\max}(\gamma)=\frac{1}{b}\int_{\infty}^{\gamma}\frac{d\gamma'}{\left(\gamma'-\frac{\alpha}{2b}\right)^2+\left(\frac{\mu}{2b}\right)^2}, \quad \text{(A24)}$$

or

$$t_{\max}(\gamma)=\frac{\pi}{\mu}-\frac{2}{\mu}\arctan\frac{2b\gamma-\alpha}{\mu}. \quad \text{(A25)}$$

It can be shown that at $t_{\max}$, $n(\gamma,t)$ reaches its first maximum. This follows from the fact that $Q(\gamma)$ is given by a negative power law and from the result that

$$\lim_{t\to t_{\max}} h(\gamma,t)=\infty. \quad \text{(A26)}$$

This result would not be true for a production rate with a positive power-law form.

Beyond $t_{\max}$, $n(\gamma,t)$ decreases toward zero. We therefore adopt the solution attained at $t=t_{\max}$ as the appropriate steady-state solution. Thus,

$$n_s(\gamma)=\frac{1}{k-\alpha\gamma+b\gamma^2}\exp\left(\frac{2\lambda}{\mu}\arctan\frac{2b\gamma-\alpha}{\mu}\right)\int_{\gamma}^{\infty} Q(\gamma')\times\exp\left(\frac{-2\lambda}{\mu}\arctan\frac{2b\gamma'-\alpha}{\mu}\right)d\gamma'. \quad \text{(A27)}$$

Again the integral in Eq. (A27) cannot be evaluated in a closed form for arbitrary λ. For the case $\lambda\to 0$ (or $\lambda\ll\mu$), we can write

$$\lim_{\lambda\to 0} n_s(\gamma)\equiv n_s(\gamma)=\frac{1}{k-\alpha\gamma+b\gamma^2}\int_{\gamma}^{\infty} Q(\gamma')d\gamma'. \quad \text{(A28)}$$

Finally, the solution for $\alpha\to 0$ follows from Eq. (A27), or from (A28) if $\lambda\to 0$, *unless* $b=0$. In that case we again solve Eq. (A1) and find

$$n(\gamma)\,|_{b=0,\alpha=0}=\frac{\exp(\lambda\gamma/k)}{k}\int_{\gamma}^{\infty} Q(\gamma')\times\exp\left(\frac{-\lambda\gamma'}{k}\right)d\gamma'. \quad \text{(A29)}$$